Mixing carbon nanotubes with asphalt binder through a foaming process toward high-performance warm mix asphalt (WMA)

Mehdi Zadshir^a, Fangliang Chen^a, Xiaokong Yu^a, Xin He^a, Irene Nigro^b, Maddalena Ricciarelli^b, Filippo Ubertini^b, Huiming Yin^{a,*}

- *Corresponding Author
- ^a Department of Civil Engineering and Engineering Mechanics, Columbia University 610 Seeley W. Mudd 500 West 120th Street, New York, NY. 10027. USA
- ^b Department of Civil and Environmental Engineering, University of Perugia Via G Duranti 93, 06125 Perugia, Italy

Abstract

This paper investigates a new approach to mixing carbon nanotubes (CNTs) through a foaming process to produce high-performance warm mix asphalt (WMA). It is challenging to uniformly mix CNTs in asphalt without agglomeration in the manufacturing process. The foaming process creates an opportunity to disperse CNT modifiers in the asphalt binder uniformly at a large scale for enhanced thermomechanical properties. Two different solvents of ethanol and a water-based surfactant are used to disperse the multi-walled CNTs. Initial morphological assessment of the two CNT solutions showed that while ethanol caused the CNTs to agglomerate, a more homogenous dispersion of the CNTs was achieved using the water surfactant solution. The foaming performance, thermal, and rheological properties of the foamed asphalt mixed with different amounts of CNTs are further investigated. The test results showed that a very small amount of CNTs $(0.06\% \sim 0.1\%)$ in weight of the binder) could effectively enhance the foaming performance for bubble stability without tangibly increasing the rheological properties of the foamed asphalt. The specific heat capacity of the foamed samples was smaller than the neat binder, whereas the glass transition temperature of the foamed samples shifted to a lower temperature as compared to that of the neat binder. The thermal conductivity of the 6% CNTs sample (0.24% wt. in asphalt binder) was improved by a two-fold mechanism compared with the foamed unmodified asphalt, which indicates the potential of using CNTs in the binder for enhancement of thermal properties in asphalt pavements.

Keywords: Asphalt Foaming Process, Carbon Nanotube (CNT), Asphalt Binder, Warm Mix Asphalt (WMA), Rheological Properties

1. Introduction

In the past decades, due to a dramatic increase in traffic loads, pavement agencies and industries are facing the need to exchange the traditional pavement materials with new ones that have higher quality, meet current safety standards, and are more reliable as well as environmentally friendly. During the paving process, a large amount of greenhouse gasses and other emissions are generated in the form of blue smoke, which consists of very small oil droplets that come from asphalt or reclaimed asphalt pavement (RAP) materials at high temperatures. To address the issues faced by the asphalt paving industry with regards to higher energy costs and environmental impacts from the production of traditional hot mix asphalt (HMA), warm mix asphalt (WMA) has been adopted in Europe and the United States in the past two decades [1-3].

WMA is a group of technologies used for asphalt pavement produced and placed at lower temperatures than those used for conventional HMA [4]. Through various chemical additives, surfactants, foaming methods, and non-foaming additives, WMA attempts to improve the workability and reduce the viscosity of the asphalt binder [5-7]. This allows the asphalt binder to be absorbed by the aggregates at temperatures lower than those used in traditional HMA production. Recently, WMA produced by water injection has gained increased popularity among asphalt producers since it does not require the use of costly additives and involves a relatively inexpensive one-time plant modification. According to the annual asphalt pavement industry survey, plant foaming accounted for more than 88 percent of the WMA in the market in 2012 [8].

Water-based foaming asphalt is produced by injecting cold water into hot asphalt binder. The water is turned into vapor and trapped in numerous tiny bubbles in the asphalt, which causes spontaneous foaming and greatly increases the volume of the asphalt [7, 9, 10]. This foaming process significantly increases the volume of asphalt binder with a large surface area [11]. When foamed asphalt mixes with aggregates, a strong coating with a high shear strength of the mix can be generated. In addition, since foamed asphalt is flexible and has a larger volume, its workability is considerably improved. Therefore, WMA can be manufactured at a lower temperature within a shorter period of time and the optimum asphalt content of a foamed asphalt mix is lower than that of the non-foamed one. Because of this, the WMA generated with water-based foaming asphalt

has various advantages over traditional WMA or HMA such as reduced binder cost, shorter production time, lower energy consumption, more environmental benignancy, and broader applicability [12-14].

From the engineering point of view, an ideal asphalt binder should be able to sustain resistance to multiple types of distresses. In particular, it should possess: (1) high relative stiffness at high service temperatures (summer) to reduce rutting, which is a distortion caused by an instability of the asphalt pavement, and shoving (the formation of ripples across asphalt pavements); and (2) increased adhesion between asphalt and aggregates in the presence of moisture to reduce stripping, meaning the loss of the bond between asphalt and aggregates due to moisture [15, 16]. However, in water-based foaming asphalt, some vapors resulting from the injected water in the hot binder may be caught in the asphalt in the form of little bubbles, which could soften the original binder and as a result, make the foamed asphalt binder susceptible to permanent deformation. Thus, further modifications of the foamed asphalt would be recommended to compensate for the softening issue.

In recent years, many researchers have tried the use of organic and inorganic additives such as polymers, nanoclay, nanofillers, crumb rubber, fibers, bio-rejuvenators, etc., to improve different physical and rheological properties of asphalt binder as well as asphalt mixture [17-22]. Nanoparticles, on the other hand, owing to their small size and large surface area, exhibit some unique features and properties that make them suitable candidates to be used as additives in the field of asphalt pavement.

One recent study examined the rheological and physical characteristics of nanoclay in both asphalt binder and mixture and found that the addition of 1 to 4 % of nanoclay can reduce the penetration and softening point while increasing the rutting and fatigue resistance [16]. Other researchers have used different nanoparticles such as nano-carbon, carbon nano-fiber, nano-ZnO, nano-SiO2, and nano-TiO2 to improve mechanical, rheological, anti-aging, thermal, and electrical conductivity, as well as the chemical bonding between the aggregates and binder [23].

The use of 10 to 40% graphite in asphalt binder has shown an increase of up to two folds and a half in the thermal conductivity values of asphalt binder [24]. This is of particular interest in systems such as hydronic asphalt pavement (HAP) where a series of serpentine or parallel pipes are embedded beneath the pavement's surface or in the base layer and a mixture of water plus an anti-freeze is circulated in them to deice the snow and ice in the winter and collect energy or cool

the overlay in the summer [25]. However, the low thermal conductivity of asphalt materials hinders the effectiveness of the heat exchange. Yu et al. [26] evaluated the feasibility to add CNTs or graphene nanoplatelets (GNPs) for enhanced thermomechanical performance and found that CNTs can be more effective when the same weight percentage is used compared with the GNPs.

Among the various nanomaterials, carbon-based nanoparticles and platelets have also received great attention in recent years due to their exceptional properties. In particular, CNTs represent the most promising additive to enhance the performance of structural and construction materials. For example, the Young's modulus of CNTs can be as high as 1000 GPa [27] and the tensile strength can reach 150 GPa [28], in addition to high thermal conductivity, theoretically almost 6 times of copper, and low electrical resistivity compared with commonly used materials [29]. However, one challenge is that no pure material can be made from CNTs that present these values. Thus, CNTs and carbon nanoparticles have been mostly mixed with polymers such as asphalt binder and elastomer matrices in the composite form.

Extensive studies have been conducted by applying CNTs in pavement engineering. It was found that when CNTs are added with a sufficiently high weight percentage in the base asphalt binder, they can significantly affect rheological properties. This mixing ratio was originally found to be > 1% [30, 31] and then reduced to 0.5% [32]. It was also found that adding 0.1% wt. of CNTs, with respect to bitumen, into asphalt mixtures in addition to improving asphalt pavement properties, decreases the required thickness of the under layers and as a result, reduces stone material consumption [33]. Furthermore, CNTs have the potential to provide an enhancement of low-temperature cracking and rutting resistance [34-36]. Moreover, the susceptibility of CNT-modified asphalt to oxidative aging could be reduced in the long-term performance of bituminous mixtures [37].

The inclusion of CNTs in asphalt binders also changes their physical and chemical properties. The relation between the modification of binder with CNTs and improvement in the rutting factor, fatigue life, and fracture resistance has been documented [38, 39]. However, it has been shown that a low percentage of nanoparticles (less than 0.2% wt.) did not have significant effects, while with 1%, there is an increase of one level of PG grade (6°C). Thus, at least 1% carbon nanoparticles by weight of the binder are needed to increase the complex modulus, elastic modulus, and viscous modulus values of the binder as well as the rutting factor [35]. The antiaging potential of using CNTs in asphalt has shown that the addition of the nanotubes can decrease

the oxidative aging of the neat binder [32] and Styrene-Butadiene-Styrene (SBS) polymer-modified asphalt by working as a barrier that prevents the diffusion of oxygen in the asphalt system [40, 41].

A uniform dispersion of CNTs in asphalt binder is essential to effectively improve the mechanical and rheological properties of the modified asphalt. However, because of the extremely high aspect ratio of the CNTs, the strong Van der Waals attraction force between nanotubes often results in the formation of bundles, ropes, and agglomerates, which makes it very challenging to uniformly disperse CNTs in the polymer matrix [42]. The dispersion quality of CNTs in the asphalt matrix significantly affects the properties of CNT-modified asphalt [34].

Different mixing techniques result in different dispersion qualities of the CNTs in the asphalt matrix and hence the mechanical and rheological properties of the modified asphalt. By adding 3% CNTs (weight of asphalt), the impact of different mixers on the mixture conditions of asphalt and CNTs was investigated and the results showed that the high shear mixer yields more homogeneous asphalt than the mechanical stirrer and that the ultrasonic mixer creates the best form of asphalt-CNT mixture [43].

Khattak et al. studied the effect of carbon nanofibers in asphalt binder using both wet and dry methods [31]. In the wet method, the nanomaterial is first dispersed in a solution and then added to the asphalt binder, whereas in the dry method (also known as the simple method), the nanoparticles are directly added to the binder via mechanical shear mixing. The results showed that the modified asphalt binder with nanofibers through the wet process had a slightly lower rutting resistance ($G^*/\sin\delta$) compared with the neat binder, whereas the dry mixing process increased the rutting resistance factor by up to 47% [31]. This could be attributed to the higher agglomeration of the nanomaterials in the dry method compared with the wet method, thus, resulting in a higher value of the complex modulus of the samples.

A wet process applied commercial kerosene as a solvent to disperse the CNTs and then mixed it with asphalt binder [44]. The CNTs were dispersed in the solvent by sonication and high shear mixing. Although the mixing process increased the dispersion quality of CNTs, it negatively affected most of the mechanical and rheological properties of asphalt due to the use of kerosene solvent with asphalt. Thus, it was concluded that the wet mixing process is more complicated and not feasible from an economical point of view [34, 44].

Another research on the comparison of the two methods showed that while the dry process of mixing multi wall carbon nanotubes (MWCNTs) with asphalt binder resulted in higher softening point and viscosity, it also caused some large accumulated particles as evaluated by the use of scanning electron microscopy (SEM), whereas, by using the wet process, CNTs distributed more uniformly in the matrix and less agglomeration of particles was observed [44]. It has also been documented that the wet-mix process, even if it is more complicated and expensive, works better than the simple mix process such that 1% of CNT addition can increase the asphalt binder's viscosity 1.5 times, thus increasing the rutting resistance and the tensile strength to reduce the thermal cracking [45].

The recent work [26] conducted the laboratory investigation of CNT-modified asphalt binders for the improvement of thermomechanical behavior for HAP applications. Hand, mechanical, and ultrasonic mixing were used to thoroughly mix CNTs with the asphalt binder. In actual asphalt concrete production and construction, it is important to scale up the laboratory-based process to fit actual asphalt mixers in field plants. To improve the method, CNTs can be firstly mixed into water with the surfactant for a uniform suspension, then be introduced into the water-based asphalt foaming process, which can facilitate both phase change of water and vapor/CNT mixing simultaneously, and finally be used for hot mix asphalt (HMA) or warm mix asphalt (WMA) production.

The findings of numerical simulations using the smooth particle hydrodynamics (SPH) aligned well with the experiments showing that the maximum expansion ratio has a linear relation with the pressure in the functioning chamber and that the temperature does not have a tangible influence on the foaming evolution and its characteristics [11], in which 0.1% wt. was the maximum content of MWCNTs admitted by the foamed process to avoid the overdose of the foaming agent of the CNT-water suspension.

Currently, almost all of the modified asphalt binders have been prepared by mixing the pure binder with fillers using either a mechanical stirrer, high shear mixer, ultrasonic mixer, or a combination of them. It is possible to achieve a uniform mixture if the filler's aspect ratio is close to 1 such as carbon black. However, it will be extremely difficult to uniformly disperse the filler in the binder when the filler exhibit a large aspect ratio >100 such as nanotube, nanofiber, or graphene nanoplatelets because they tend to entangle together in the binder.

This study explores an efficient manufacturing process to produce high-performance WMA by mixing CNTs through asphalt foaming, and the possibility of adding higher dosages of CNTs to the asphalt binder is investigated. An in-house nozzle-based foamer is used to produce foamed asphalt uniformly mixed with CNTs. The foaming performance and rheological properties of the foamed asphalt mixed with different percentages of CNTs are further investigated. Solutions of MWCNTs with 0%, 1%, 1.5%, 2%, 2.5%, 3%, and 6% wt. of the solvent are prepared and used as the foaming agent to foam the asphalt binder. Then, different tests are performed to look at the morphology of the disseminated CNTs and measure the rheological and thermal parameters of the samples of the foamed asphalt binder that are modified with CNTs.

2. Materials and Methods

2.1. Asphalt Binder

In this study, two asphalt binders with the Performance Grade (PG) 64S-22 and 70-22 were calibrated, and eventually, the PG64S-22 provided by Peckam Industries Inc. (the Bronx, 10466 NY) was used for all experimental tests. The material has been tested and certified to be in conformance with AASHTO requirements and applicable to NY, NJ, PA, or New England Department of Transportation (DOT) specifications. The binder which is polymer modified meets the elastomeric properties required by AASHTO MP19 & TP70. It is also certified that the product has no motor oil constituents. The material properties of the neat asphalt binder are shown below in Table 1 Table 1.

Table 1 Specifications of the Neat Binder Used in This Study.

PG classification	PG64S-22
Penetration	65
Elastic Recovery	0.00
Mix Temp Max/Min °C	164/157
Compaction Temp Max/Min °C	151/146
Viscosity @135°C (275°F) Pa.s	0.493
Viscosity @165°C (329°F) Pa.s	0.135
Specific Gravity @15.6°C (60°F)	1.043
Specific Gravity @25°C (77°F)	1.037
Modifiers	None
Additives	None

2.2. Multiwall Carbon Nanotubes (MWCNTs)

Two different types of CNTs are widely applied: single tubes (single-wall CNTs) and coaxial multiwall tubes (MWCNTs). MWCNTs are less expensive and easier to produce but exhibit lower strength and stiffness than single-wall CNTs [46]; thus MWCNTs are applied in this study. The US4315 MWCNTs were purchased from US Research Nanomaterials, Inc. The MWCNTs have an outer diameter of 50-80 nm, an inner diameter of 5-15 nm, and a thickness of 45-65 nm. As the distance between each wall is about 0.34 nm, the number of layers ranges from 45/0.34=132 to 65/0.34=191. Table 2Table 2 summarizes the relevant properties of the MWCNTs. Throughout this paper, the MWCNTs is shortened to CNTs for simplicity.

Table 2 Specifications of the MWCNTs Used in This Study.

Properties	MWCNTs
Purity	>95% purity
Outside diameter	30-50 nm
Inside diameter	5-15 nm
Length	10-20 um
Color	Black
True density	2.1 g/cm^3
Stock#	1231YJ
C	97.37%
Cl	0.20%
Fe	0.55%
Ni	1.86%
S	0.02%
Aspect Ratio (diameter/length)	2.67E-03

2.3. Preparation of CNT Solution

The CNTs being at the nanoscale, are characterized by a large surface area. Therefore, because of their extremely high aspect ratio, the strong Van der Waals attraction forces between the nanotubes often result in the formation of bundles, ropes, and agglomerates, which makes it very challenging to uniformly disperse them in the polymer matrix [42]. As mentioned before, studies have shown that the wet mixing process results in a more uniform dispersion of the nanoparticles. Thus, in this study, the CNT solutions were made by following the wet process, which uses a solvent to well disperse the CNTs initially in a solution, and then in the asphalt binder. Researchers have tried

different solvents such as kerosene [31, 44], acetone [47], varsol, and turpentine [23] to implement the dissolution of the CNTs and mix them with asphalt.

In this paper, two different CNT solutions are prepared, one using ethanol, and the other with a commercial dispersant. For the first solution, ethanol was used as the diluent and the dispersant for the CNTs, and solutions with 3% and 6% CNTs by weight of the ethanol with the same volume were made. To prepare the solutions, after adding 60 ml of ethanol to a glass beaker, the weighed CNTs were added to the beaker and were hand mixed with a stirrer. To complete the mixing process, a Sonic Dismembrator (also called Ultrasonic Processor) No. FB-505 model was utilized to mix the components with an amplitude of 90%, 1s pulse on and 1s pulse off at 500W for 30 minutes. During the ultrasonic process, the beaker was placed in an ice bath and the temperature of the CNTs-ethanol solution was constantly monitored to avoid overheating and prevent the ethanol from evaporation (the boiling temperature of ethanol is about 78°C) (Figure 1Figure 1).

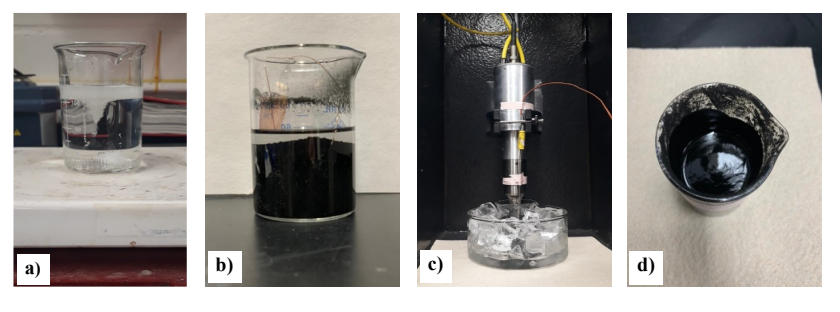


Figure 1 Dispersion procedure to prepare the CNT solution: a) initial ethanol; b) CNT powder added to the ethanol; c) sonication with an ice bath; d) final CNT solution.

For the second solution, deionized (DI) water was used and in order to facilitate the dispersion of CNTs in DI water and improve the separation of particles in an aqueous solution, a surface-active dispersing agent (surfactant) of US4498 was used that was purchased from the US Research Nanomaterials (Huston, Texas 77084, USA). This is a non-ionic surfactant that contains aromatic groups. The aromatic groups result in good affinity and easily adsorb on the wall of the nanotubes. The agent has 90% active substance content and 10% moisture (water) content with a cloud point of 68-70°C. Based on the supplier's experimental results, US4498 is particularly suitable for carbon nanotubes to be dispersed in water.

First, the water dispersant was mixed with DI water. The mixing ratio of the dispersant and the CNTs was chosen as 0.1:4 in accordance with the instructions from the supplier. To better dissolve the dispersant which has a jelly texture, a magnetic stirrer was used for mixing for 10 minutes. Once the dispersant was completely dissolved in the DI-water, the already weighed CNTs were added to the solvent. Then, the sonication process was performed similarly to the ethanol-based sonication mixing.

In order to prepare foamed asphalt samples with different concentrations of CNTs, the distilled water with different percentages of CNTs (0%, 1%, 1.5%, 2%, 2.5%, 3%, and 6%) were prepared. All the percentages presented in this study are regular weight percentages (wt.%) to simplify the notation. Figure 2Figure 2 illustrates the detailed procedures of preparing a well-dispersed CNTs solution as recommended by the supplier.

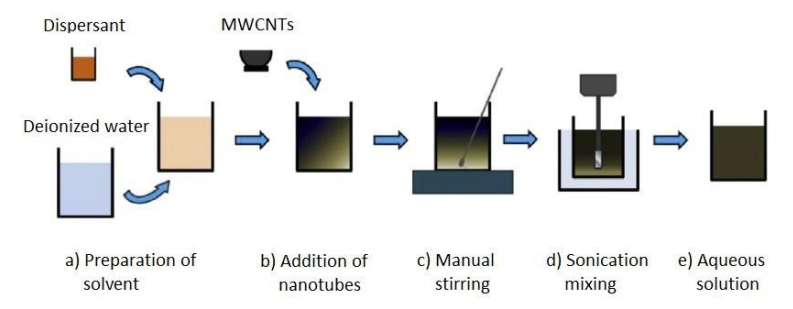


Figure 2 Illustration of the dispersion process of the CNTs in distilled water.

At the end of the mixing process, for a more in-depth and methodological evaluation of the homogeneity of the solutions, some preliminary studies on the morphology of the samples were done using a scanning electron microscope (SEM) to determine which solvent resulted in less agglomeration of the CNTs and a more uniform solution.

Afterward, a series of tests were conducted to investigate the foaming performance and rheological properties of the foamed binders mixed with different amounts of CNTs, such as the foaming indicators, viscosity, and complex modulus.

2.4. Foaming method

The foaming method is accomplished by spraying a small amount of liquid foaming agent (either pure distilled water, ethanol-based CNT solutions, or commercial dispersant-based CNT solutions) into the binder via a nozzle embedded in the wall of the functioning chamber. When the

hot binder comes into contact with a liquid droplet at the ambient temperature, it exchanges energy with the surface of the liquid droplet by heating the droplet to a vapor state. This process results in explosive expansion of the droplets and generates a large amount of steam bubbles. The steam bubbles are forced into the continuous phase of the binder under air pressure in the expansion chamber. With emission from the spray nozzle, the encapsulated steam expands until a thin film of a slightly cooler binder holds the bubble intact through its surface tension. This process occurs for a multitude of asphalt bubbles and thus, produces a foamed asphalt binder.

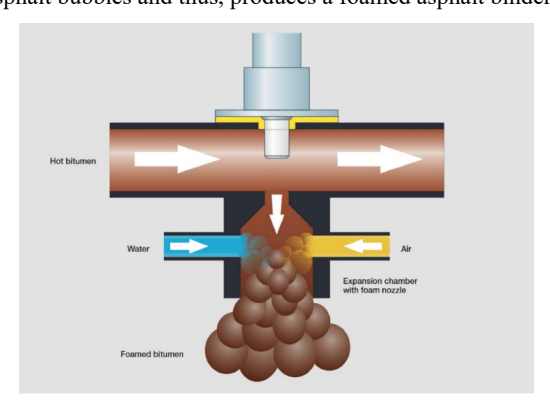


Figure 3 Schematic illustration of asphalt foaming process (Wirtgen Group, 2009)

Originally, the experiments were performed using a commercial foamer to foam the asphalt binder, but it often suffered from clogging of the foamed asphalt in the water tubes. Thereafter, an in-house foaming machine shown in Figure 4 was developed to generate the foamed asphalt binder. For this foamer, a high-speed long-range Laser Displacement Sensor (LDS) is used to characterize asphalt foaming properties and obtain the expansion ratio, half-life, and foaming index. The LDS sends a pulse of laser light to a target surface and detects the reflection with an accuracy of 0.02%. A container with a dimension of 4" (diameter) × 8" (height) is placed under the front outlet at a location where the laser light is aligned with the center of the container. The LDS is equipped with the LabVIEW software and configured with a 5Hz sampling frequency which makes the LDS capable of capturing detailed information about the foaming evolution. The developed LDS is integrated into the foaming machine and is designed to measure the foaming evolution automatically throughout the entire foaming process. It avoids any operational errors and thus provides objective, automatic, highly accurate, and repeatable measurements.

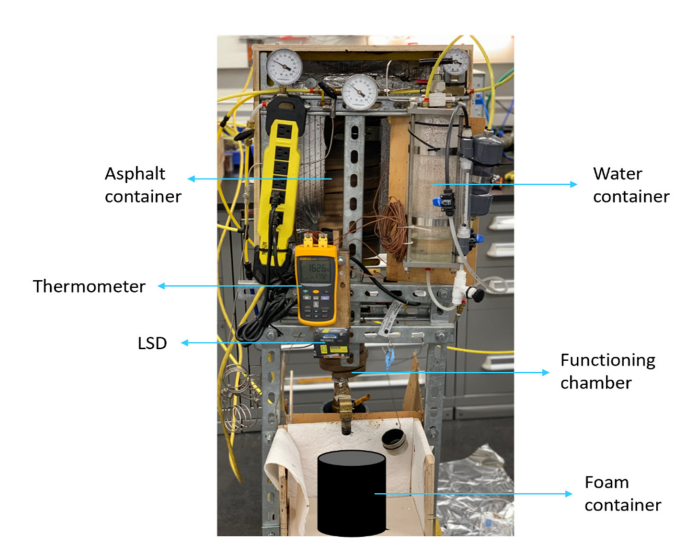


Figure 4 Components of the in-house foaming machine.

The foaming machine is connected to an air injector that can run with a pressure of 0 to 80 psi (0.55 MPa) using a regulator. To control the flowing rate of the foaming agent, both the flowmeter and the foaming barometer can be used. Under a constant air pressure of 80 psi in the foaming agent barometer, the foaming agent flow capacity ranges from 0 to 45 ml/min and is adjusted using the flow switch. The binder container has a capacity of 1 gallon and governs its temperature using the asphalt heater band surrounding the binder container. With a full load, the heater can sustain a fully filled tank of binder up to 240°C. The binder container is connected to the functioning chamber via an adjustable valve with a marker.

The functioning chamber (also known as the expansion chamber) is where the foaming happens. In order to foam the asphalt, both air and a foaming agent are required, where the foaming agent could be water, ethanol, or as in this study, a CNT solution. The flow rate of the binder from its container to the functioning chamber is controlled with both the asphalt flow barometer and the adjustable valve. At a fixed position of the valve, the larger the air pressure applied in the binder container, the higher the flow rate of the binder to the functioning chamber will be obtained. The injectable air inlet and foaming agent nozzle are located on the two opposite sides of the functioning chamber. The position of the air inlet is slightly higher than that of the nozzle such that the foaming agent spray injected by the nozzle will react with the high-temperature binder a

little longer in order to generate more bubbles in the binder. The flow rate system configured in this setup can control the flow rate of the injected solvent down to 2 ml/min with an accuracy of 1% and has a much higher resolution than that of the commercial one.

Similar to that of the binder container, the temperature of the functioning chamber is controlled by the other heater band. Under a constant injected air pressure, the temperature in the functioning chamber changes with the flow rate of the foaming agent spray. It was found that under a constant air pressure of 50 psi (0.34 MPa) and a constant water spray flowing rate of 20 ml/min, the maximum temperature in the chamber is able to maintain at about 250°C.

The temperature in both the binder container and the functioning chamber is measured through the thermocouples installed in their center positions and displayed in the digital thermometer. The thermal system of the in-house foamer is covered by a thermo-isolated case to save more thermal energy and achieve a more stable thermal status.

The foaming nozzle is calibrated before running the foaming machine by employing the volume and the time duration of the test to measure the flow rate per pressure of the nozzle. The flow rate of the nozzle is about 63 ml/min at a pressure of 40 psi. In order to perform the foaming, the temperature of both the binder container and the functioning chamber has to be set close to 150±5°C and remain stable for at least 10 minutes, and the pressure is set to be 25 psi for both chambers. By doing the calibration, it is possible to correlate the pressure with the representing flow rate, and this is necessary to estimate the exact ratio between the asphalt binder and the foaming solution. In the end, the ratio of CNTs to asphalt can be utilized to calculate the percentage of CNTs in the asphalt binder, which can be easily calculated by using Eq. (1):

% wt. CNTs in binder = (% wt. CNTs in solution)
$$\times (\frac{foaming \ agent}{binder})$$
 (1)

As explained above, the mixing process of the binder and the foaming solution happens in the bottom chamber of the foaming machine. The dispersions with different amounts of CNTs were then added to the liquid container as shown in Figure 4. Since the CNTs are assumed to be well dispersed in the solution, it is highly likely that the CNTs will be uniformly distributed in the foamed asphalt binder generated via the foaming method.

It has been found that the foaming agent content (water ratio) added to the asphalt plays a significant role in affecting the foaming performance and the rheological properties of the foamed asphalt [10]. To exclude this water ratio effect on the foaming performance of the foamed asphalt, a 4% water/binder ratio was chosen to generate the foamed asphalt. The foamed asphalt with CNT

samples were poured into a cylinder container underneath the functioning chamber. Therefore, since the percentage of binder flow is determined by the switch between the two chambers, the flow rate of the asphalt will be about 1016 ml/min. Thus, to gain a 0.04 ratio, the flow rate of the foaming agent must be 40.659 ml/min, which is achievable by setting the pressure to 45 psi for the foaming agent barometer.

Using the different weight fractions of CNTs in the water and the applied water/binder ratios, foamed asphalt samples with seven different concentrations of CNTs (0%, 0.04%, 0.06%, 0.08%, 0.1%, 0.12%, and 0.24%) were prepared, and three replicas were made for each concentration. The foamed asphalt binder (FA) with no additive just distilled water and the neat asphalt binder (NA) will be used in the experimental tests as reference samples for comparison.

Because of the low weight percent of CNT used in the CNT solution, we assume that the density of the CNTs solutions is close to the density of water. Thus, we use the same barometer settings during asphalt foaming using the CNT solutions. For example, with a foaming agent to binder ratio of 4%, a 1% wt. of the CNT solution results in the 0.04% by weight (i.e., $1\% \times 4\% = 0.04\%$ according to Equation 1) of CNTs in the asphalt binder, or by using the highest 6% CNTs solution as a foaming agent result in 0.24% by weight of CNTs in the foamed asphalt binder. The FA samples have 0% wt. of CNT. The nomenclature for the samples in this study is as follows: NA (neat asphalt binder), FA_CNT (foamed asphalt binder), and the percentages of the CNTs are shown in parenthesis.

2.5. Foaming characterizations

The characteristics of foamed asphalt significantly influence the mixture's workability and performance. Therefore, in order to effectively use the foamed binder to produce WMA, it is important to understand the characteristics of foamed asphalt with different amounts of CNTs.

Since the bubbles are thermodynamically unstable in the foamed asphalt, it is crucial to quantify their evolution with time. Current methods for evaluating foaming characteristics of foamed asphalt are based on measurements of two primary parameters: expansion ratio (ER), the increase in volume relative to the original asphalt volume, and the ratio of maximum foamed volume to the original volume of liquid asphalt is known as the maximum expansion ratio [48-50]. Accordingly, half-life (HL) is defined as the time in seconds that asphalt foam requires to collapse from the maximum expansion to half of the maximum expansion value [49, 50] (see Figure 5Figure 5Figure

5). Empirically, the parameter ER is related to the viscosity and surface energy of the asphalt binder thus affecting how foamed asphalt disperses in a mix.

In particular, ER is expressed as [12, 51, 52]:

$$ER(t) = \frac{V(t)}{V_0} \tag{2}$$

where

V(t): the expanded volume of the foamed asphalt over the time

 V_0 : the initial volume of the asphalt liquid before foaming

When the expanded volume reaches the maximum, the expansion ratio is at its maximum. Also, the assumption is that the final volume of the foamed asphalt after a long period will reach its initial volume (V_0) . Thus, the expansion ratio will be ER = 1 when $t \to \infty$.

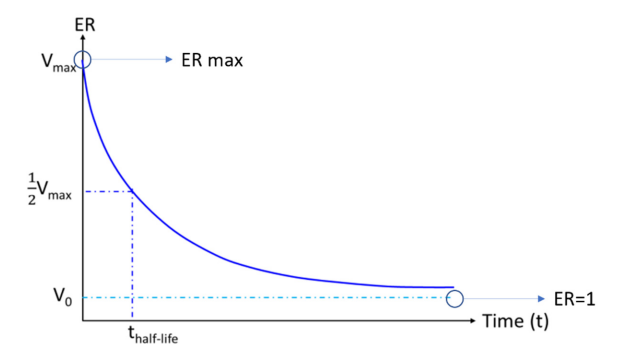


Figure 5 Evaluation of foaming characteristics.

HL is a measurement of the foamed asphalt stability. It provides an indication of the rate at which the foamed asphalt bubbles collapse with time, which in turn, determines the length of time the foamed asphalt will remain in the foamed state to allow enough time for coating aggregates in a mix. The definition of HL thus reads as [12, 51]

$$HL = t|_{V = \frac{V_{max}}{2}} \tag{3}$$

which is the time (in seconds) at which the overall foam volume is reduced by half from its maximum value. In other words, this is the time (t) that the foaming volume reaches half of the maximum expansion volume.

Another parameter that is gaining wide application in qualifying the characteristics is the foaming index (FI), a measurement of the area under the decay curve (i.e., the change in expansion ratio with time) that reflects the stored energy in the foam for a specific foamed asphalt at a known temperature and a determined application rate [12, 51, 52]:

$$FI = \int_{t=0}^{t|_{ER=1}} [ER(t) - 1]dt \tag{4}$$

which can be numerically integrated by the sum of the area for many time steps. Here $t|_{ER=1}$ indicates the time that asphalt is completely stabilized at the initial volume with ER=1.

2.6. Characterization of the rheological properties of the foamed asphalt with CNTs

To evaluate the effects of the added CNTs on the foamed asphalt (FA) binders, the rheological properties of the pure asphalt and FA with different amounts of CNTs were tested with the Dynamic Shear Rheometer (DSR).

2.6.1 Viscosity tests

The dynamic viscosity tests were conducted by applying constant shear stress with a defined temperature domain via the Viscometry Module in the DSR. In this study, the viscosity of the neat (original) asphalt (NA) binder and foamed asphalt (FA) binder with different percentages of CNTs were measured across a temperature range from 90°C to 150°C. Samples were loaded in the geometry of cup and bob. The viscosity test was conducted in accordance with AASHTO T315-10 (AASHTO T315 2010), which describes the standard way to determine the rheological properties of the asphalt binder using a DSR.

2.6.2 Oscillation tests

For the rheological properties, a TA Instrument dynamic shear rheometer (DSR) was used and the AASHTO T315-10 standard with some modification was applied as a guideline for the preparation of the samples. It was not possible to completely follow the instructions in the standard due to the nature of the material studied. The presence of bubbles in the foamed samples, as well as the presence of CNTs in the modified foamed samples, could potentially affect the sample preparation, trimming, and results of the test.

The oscillation amplitude sweep test and oscillation frequency sweep test were done using the 25 mm in diameter parallel plates with a 1 mm gap. The former was used to find the linear viscoelastic region (LVE), and the latter was used to obtain the rheological parameters such as G'

(elastic or storage modulus), G" (viscous or loss modulus), G* (complex modulus) and the phase angle (δ) of the samples. For the oscillation amplitude sweep test, a temperature of 70°C was selected with the amplitude of the strain (deformation) ranging from 1 to 100 % of strain while the frequency was kept constant at 10 rad/s. Test frequencies chosen for each sample were set in the range of 0.1 to 100 rad/s (0.0159-15.9 Hz) at different temperatures: 46°C, 52°C, 58°C, 64°C, 70°C, and 76°C while 1 % strain was applied based on the outcomes of the linear viscoelastic domain.

The accuracy of the DSR measurements depends upon accurately measuring the test specimen diameter which is assumed to equal to the test plate diameter. For this reason, the trimming of excess binder and the final closure of the gap producing a slight bulge in the test sample are critical steps in the DSR test. The complex modulus, G*, is calculated using Eq. (5):

$$G^* = (2h/\pi r 4)(^{\tau}/_{\Theta}) \tag{5}$$

where τ is the torque applied to the test sample, h the thickness of the specimen, Θ the angular rotation in radians, and r the radius of the test plate.

2.7. Scanning Electron Microscope (SEM)

To better evaluate the dispersion of CNTs in each solution, a Zeiss SEM was used. A technique of dipping a toothpick into the solution and drawing lines on an aluminum plate was used to prepare the samples. Image formation in an electron microscope requires a high vacuum environment. Thus, drying the samples was a prerequisite for viewing and obtaining good images in a normal high vacuum SEM system. Creating a conductive layer of metal on the sample inhibits charging, reduces thermal damage, and improves the secondary electron signal required for topographic examination in the SEM. Therefore, the carbon coating was applied when necessary.

2.8. Differential Scanning Calorimetry (DSC)

Changes in the thermal properties (e.g., specific heat capacity Cp and glass transition temperature Tg) of all binders were evaluated using a TA Instruments Q250 Differential Scanning Calorimeter (DSC). For sample preparation, Tzero hermetic pans and hermetic lids were used to hold ~10 mg of samples. No further drying process was applied to the samples before sealing the pan. However, a replicate set of samples were placed in a vacuum oven for about 2.5 hours at 135°C (i.e., the degassing process) to remove the air bubbles trapped in the samples (CNT_FA 3% and 6% CNTs modified samples). The modulated DSC (MDSC) function was employed because

it provides greater sensitivity than regular DSC, and it allows for differentiating between reversing and non-reversing thermal behaviors in materials [53]. MDSC heating and cooling curves were obtained at different rates with a modulation period of 60 seconds and an amplitude of ±0.47°C. A nitrogen cooling system was used for cooling and the nitrogen gas was purged at a rate of 50 ml/min. All samples were subjected to the following thermal cycles: (i) initial rapid cooling: after being equilibrated at 80°C, the samples were cooled to -60°C at a ramp rate of 10°C/min and then held isothermal for 5 mins; (ii) first heating: -60°C to 80°C at 4°C/min and then held isothermal for 5 mins; (iii) first cooling: 100°C to -60°C at 4°C/min and then held isothermal for 5 mins. Specific heat and glass transition temperature was determined from the second heating (i.e., step iv) as this cycle probably gives a more stable measurement of the sample's thermal property.

2.9. Laser Flash Apparatus (LFA)

In this study, the Nanoflash LFA 447 from Netzsch Instruments was used to perform the measurements of thermal diffusivity according to the flash method and the ASTM E-1461 standard. Nanoflash LFA 447 uses a high-performance xenon flash lamp to produce the heat pulse on the rear of the sample. An infrared (IR) detector is placed on top of the sample and collects the heat that is propagated through the sample. For the measurement of thermal diffusivity, a round liquid sample holder with a 12.7 mm diameter was used. Thermal conductivity measurements were done at 40°C for all the samples. Three shots were applied to each sample at a suggested gain of 5012, which defines the power of the flash lamp, at medium pulse width with a 20-second delay. All analyses were done using the 3-layer heat loss with plus correction embedded in the Nanoflash analysis software. The instrument was first calibrated by measuring the thermal conductivity of deionized water at 25°C and the results were within 1% deviance from the literature. By using the output values from thermal diffusivity and having the specific heat (measured from DSC) and the density of the samples, the thermal conductivity of the specimens is determined. The thermal conductivity of the samples was calculated by an indirect method: first, the thermal diffusivity was measured using the flash method, and then it was multiplied by the heat capacity (measured by DSC) and density values, according to the formula below (Equation 6):

$$\lambda = \alpha \cdot C_{p} \cdot \rho \tag{6}$$

where λ is the thermal conductivity, α is the thermal diffusivity, c_p is the specific heat, and ρ is the density of the samples.

3. Results and Discussion

3.1. SEM Results

To compare the dispersion pattern of the carbon nanotube in each solvent, samples of 3% CNTs in both ethanol and DI water-surfactant solutions were prepared. The SEM images

Figure 6

(Figure 6) show that a majority of the CNTs in the 3% CNTs-ethanol solution appear to agglomerate forming a large cluster ranging between 0.5 to 6 μm, and the rest of the nanotubes are poorly dispersed. This is mainly due to the high surface area and the strong Van der Waals force between the CNTs. The uniformity of the CNT dispersion in ethanol is not acceptable according to these SEM images. On the other hand, it can be seen that in the 3% CNTs-DI water solution, most CNTs are properly dispersed with entangling to each other. Since a uniform and homogenous dispersion of the nanotubes is a necessity to form a network for enhancement of asphalt binder's thermal, electrical and mechanical properties, only the solutions of CNTs in DI water-surfactant were chosen for further experiments.

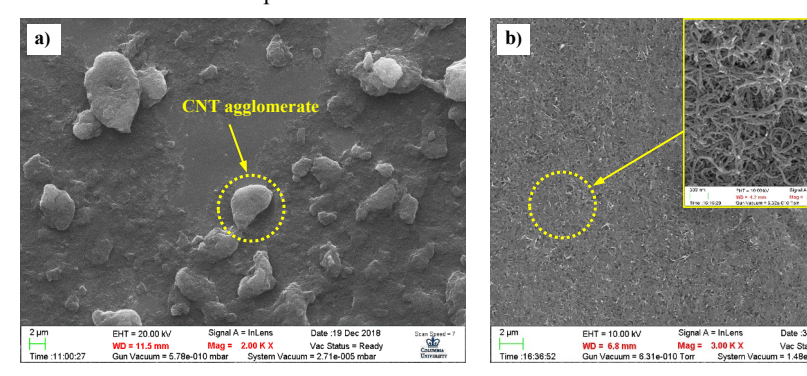


Figure 6 SEM images of CNTs in a) ethanol solution causing large agglomerates; b) DI water and surfactant solution with well-dispersed CNTs.

3.2. Foaming characterization

Typical foaming evolutions of the foamed asphalt with three different CNTs contents (0%, 0.06%, and 0.1%) are shown in Figure 7Figure 7. It shows that the foam bubbles accumulate rapidly in the container once they were ejected from the functioning chamber until a peak volume was reached within about $20\sim30$ seconds. Then, the bubbles in the foamed asphalt collapse rapidly,

Formatted: Justified

and thus its volume decreases quickly, especially for the first ~50 seconds. Thereafter, it gradually reaches a stable state with a volume expansion of about 1.2~1.5. This remaining volume is mainly due to the long-lasting small bubbles in the foamed asphalt. During the foaming process, the LDS detector in certain cases does not receive any reflection because of the mirror type dark surface of the foamed asphalt (for instance, when the laser perpendicularly hits a stilled smooth surface of the binder).

According to Eqs. (2-4), the three foaming characteristics, ER, HL, and FI, of the foamed asphalt with different amounts of CNTs can be determined, which are presented in Figure 10 Figure 10, respectively. The error bars are calculated from the standard deviation of the measurement of at least three samples. Figure 8 shows that the ER of the foamed asphalt slightly decreases as the added CNTs increase. However, the added CNTs provide a minor effect on the ER of the foamed asphalt.

In WMA applications, the HL and FI are two important parameters that indirectly relate to workability and coating. The higher the HL, the longer the foamed asphalt bubbles sustain themselves, allowing a longer time for coating aggregates in a mix. Figure 9Figure 9 and Figure 10Figure 10 show that the HL and FI of the foamed asphalt gradually increase as the CNTs increase. When CNTs were added at a small weight percentage (say 0.04% in this study), no obvious change was observed. However, when the weight percentage of CNTs reaches 0.1%, the HL and FI of the foamed asphalt increase by 45% and 28%, respectively, compared with the unmodified asphalt (CNT_FA 0%), indicating that the added CNTs, once they reach a certain level, considerably enhance the overall foaming performance of the foamed asphalt.

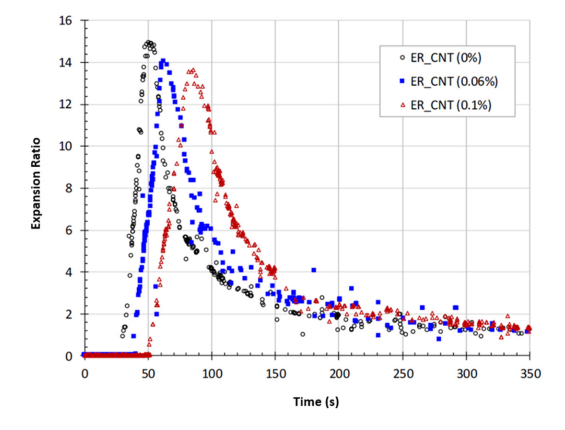


Figure 7 Expansion Ratio (ER) of the foamed asphalt with different CNTs. $\label{eq:cnt}$

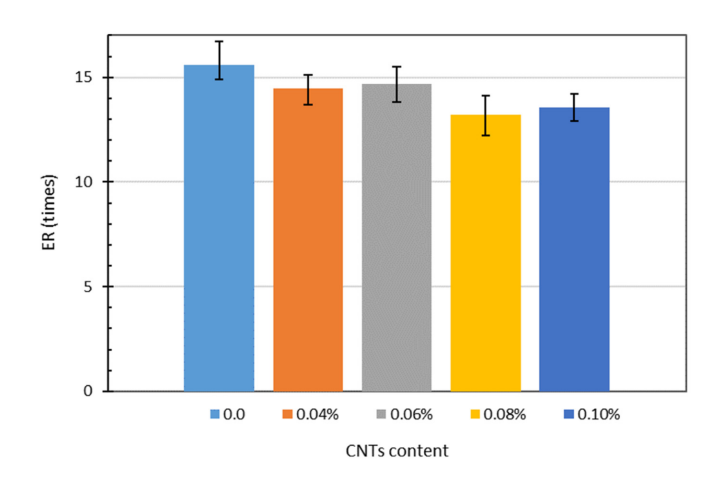


Figure 8 Comparison of ER of the foamed asphalt with different CNTs.

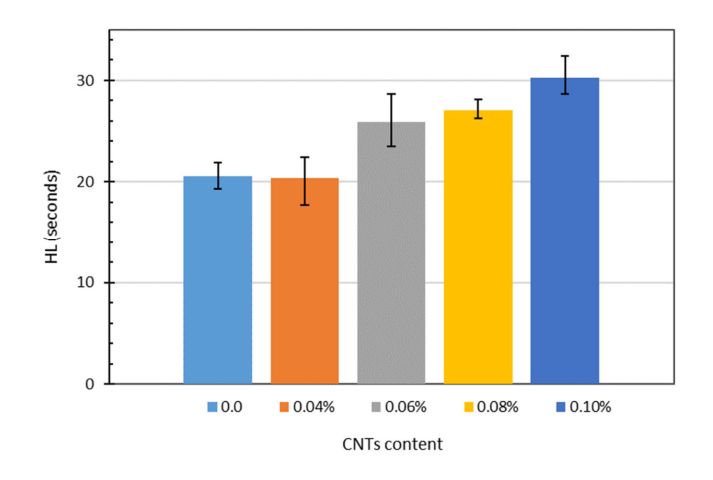


Figure 9 Comparison of HL of the foamed asphalt with different CNTs.

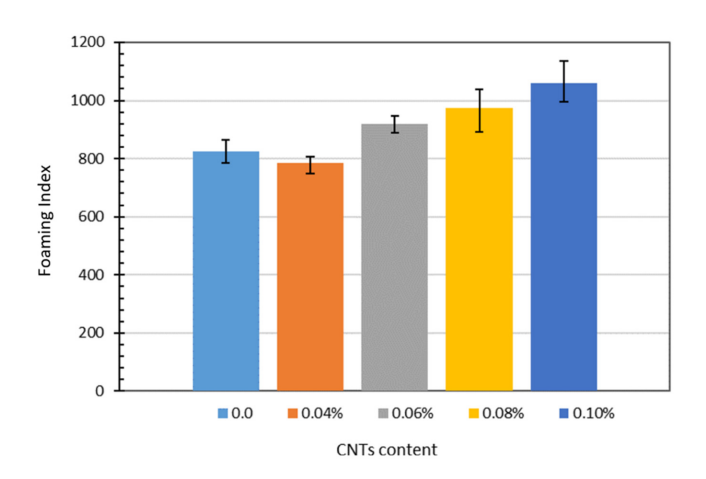


Figure 10 Comparison of foaming index of the foamed asphalt with different CNTs.

3.3. Rheological properties of the foamed asphalt with CNTs

3.3.3 Viscosity

The viscosities of different asphalt samples were measured by applying constant shear stress of 2 Pa. In this experiment, the NA binder was used as a control sample. The viscosities of the NA and FA binders with different amounts of CNTs are shown in Figure 11Figure 11. It shows that, when the temperature is lower than 120°C, the viscosities of the foamed asphalts are much lower than those of the NA while when the temperature gets higher, the viscosities of the sample were comparable to each other. The much lower viscosity of the foamed asphalt considerably eases the efforts in the mixing and compaction of WMA. Figure 11Figure 11 shows that the viscosity of the FA slightly increases as the added CNTs increase once the CNTs were added to the FA even though the difference is not apparent.

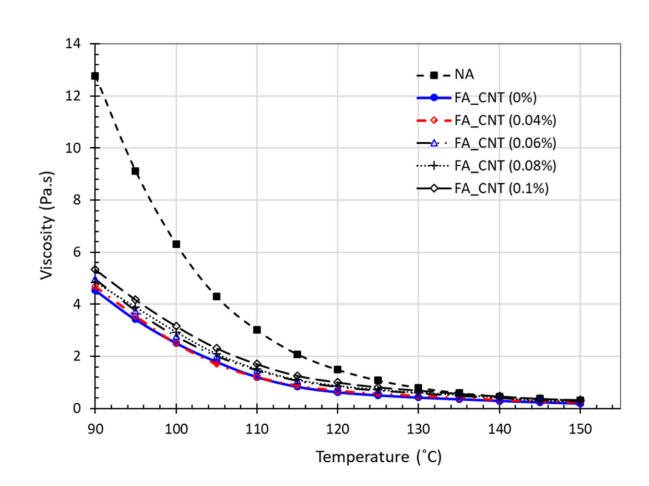


Figure 11 Viscosities of NA and FA binders with different CNTs.

3.3.4 Complex modulus and rutting performance

Figure 12Figure 12 illustrates the complex modulus of different asphalt binders. It shows that a slight softening occurs after the foaming process relative to the unfoamed condition, especially at lower temperatures. However, once the CNTs were added to the foamed asphalt, their complex moduli gradually increased as the added CNTs increased except when CNTs=0.04%. The increasing complex modulus indicates that the added CNTs enhance the resistance of the foamed binder to deformation.

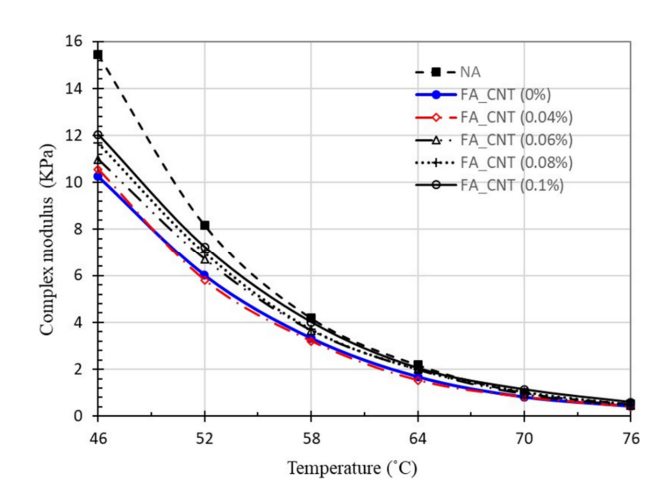


Figure 12 Complex modulus of the NA and FA with different CNTs at different temperatures.

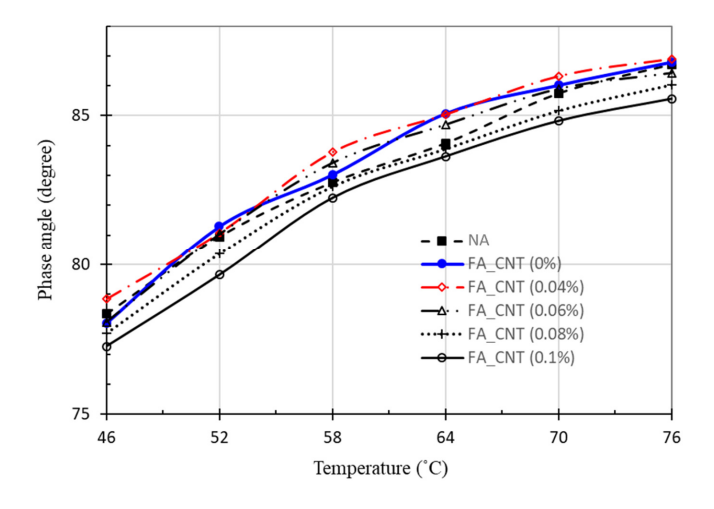


Figure 13 Phase angles of the NA and FA with different CNTs at different temperatures.

Figure 13 Figure 13 shows the distribution of the phase angle of different binders across the considered temperature ranges. By comparing the phase angle (δ) of NA and those of the FA

without or with a small amount of CNTs (0.04), no apparent trend could be found, indicating that the phase angle of asphalt material is not sensitive to the foaming process, which is consistent with the current findings in the literature [54]. Nevertheless, as the added CNTs keep increasing, a slight decrease of δ can be found in Figure 13Figure 13, which indicates that the added CNTs would make the foamed asphalt more elastic compared with conventional asphalt binder.

When the dynamic shear modulus G^* and phase angle (δ) were obtained from the DSR tests, the rutting parameter $G^*/\sin\delta$ could be calculated. According to Superpave specifications, $G^*/\sin\delta$ is a rutting factor representing a measure of the rutting resistance of the asphalt binder. In general, the higher the $G^*/\sin\delta$ in the DSR tests, the less susceptible a binder is to permanent deformation at a high pavement temperature [55]. Figure 14Figure 14 shows the $G^*/\sin\delta$ of the NA and FA with different amounts of CNTs at different temperatures. As expected, the $G^*/\sin\delta$ of all binders rapidly decreases as the test temperature increases and the difference among different binders gradually decreases. When the binder is foamed, the rutting factor decreases, however, the addition of the CNTs shows to be effective in improving the rutting factor at all temperatures, except for a small amount of the CNTs (0.04%).

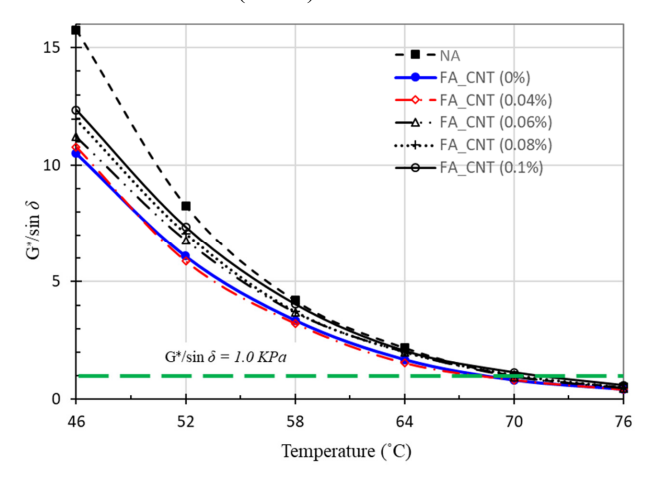


Figure 14 G*/sinδ of the NA and FA with different CNTs at different temperatures

According to AASHTO T315, $G^*/\sin \delta$ must not be less than 1.0 kPa for unaged asphalt binders, which is calibrated by the green dashed line shown in <u>Figure 14Figure 14</u>. From the intersection points of the $G^*/\sin \delta$ curves and the long dash line, the failure temperature

corresponding to a G*/sin\u00e3 of 1.0 kPa for different binders can be determined, which is shown in Figure 15Figure 15. It shows that the failure temperature of the foamed asphalt is lower than that of the original binder, and then gradually increases as more CNTs are added to the foamed asphalt, indicating that the foaming process causes a slight softening of the original binder. However, the added CNTs could enhance pavement's resistance to permanent deformation.

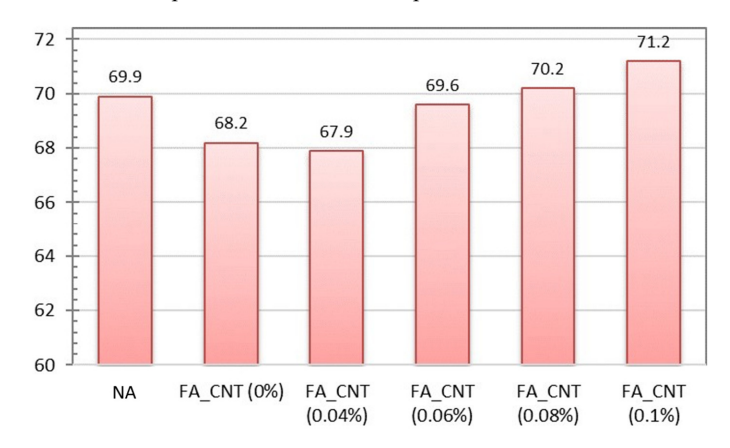


Figure 15 Failure temperatures for different binders.

3.3.5 Rheological results for samples with higher percentages of CNTs

Results of the complex moduli of the four samples NA, FA_CNT (0%), FA_CNT (0.12%), and FA_CNT (0.24%) were obtained from the frequency sweep tests at different temperatures of 52, 58, 64, 70, and 76°C and the frequency of 10 rad/s are shown in Figure 16Figure 16.

As can be seen, the samples show a similar trend for the G* values at all the temperatures except 52°C, where there is a slight difference between the moduli of the samples. As it is known, the introduction of water to the binder decreases its viscosity and thus, the foamed asphalt (FA) has the lowest moduli of all, meaning that it is less stiff. At 52°C, the 0.12% CNT foamed modified binder has a G* that was 5.2% higher compared to FA. However, as the temperature increases, the moduli of the samples tend to further overlap. The authors hypothesize that the low percentage of the CNTs in the asphalt binder did not affect the rheology of the samples at intermediate to high temperatures significantly. In addition, the prominent role of the DI water-surfactant solvent in efficiently dispersing the CNTs and lack of agglomeration can be another reason to see a similar stiffness in the modified samples.

The storage modulus (G') for the range of temperatures from 52 to 76°C with a 6°C interval and for a frequency of 10 rad/s is plotted in Figure 16Figure 16 (b). The values for storage (elastic) modulus show that the foamed asphalt (FA) has a higher modulus compared with the neat binder (NA), meaning that it is more elastic (less viscous). This could be expected because of the presence of water in the samples and its effect on lowering the viscosity. However, for the modified samples with CNT, the elastic modulus is less than the foamed samples, resulting in a relative increase of viscosity as the percentage of CNT increases from 0.12% to 0.24%. With the presence of both foam and the CNT, the viscoelastic behavior is more complicated with the competition of two reasons. Figure 16 shows the complex modulus (G*) of the 0.12% CNT foamed modified reaches the highest but the storage modulus (G') is the lowest among the four cases at 52 °C.

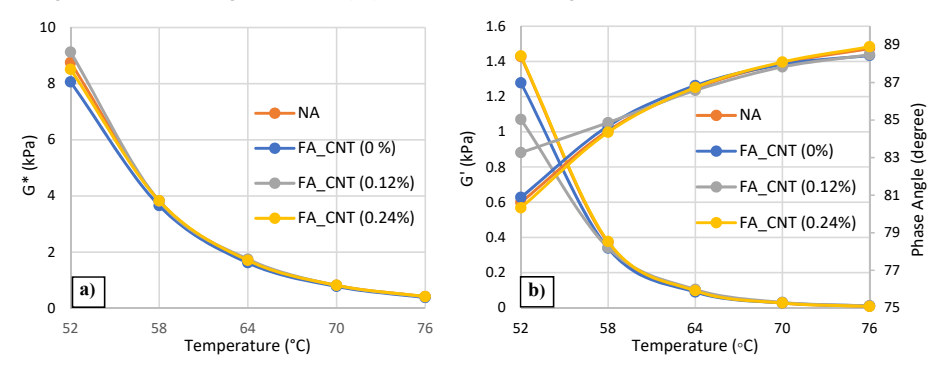


Figure 16 a) Complex modulus of all the samples at different temperatures; b) storage modulus of the samples at different temperatures.

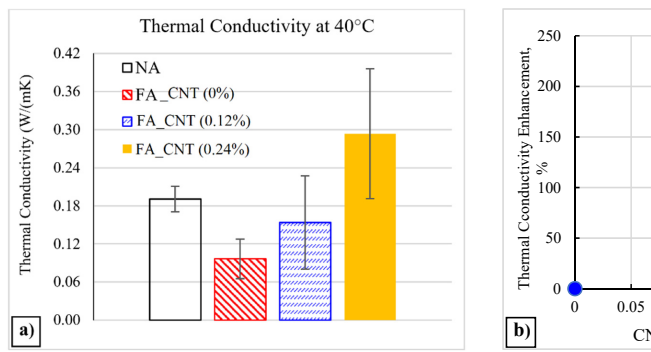
3.4. Thermal conductivity results from the LFA

For thermal analysis, only the reference samples (NA, and FA) and the modified samples with high percentages of the CNTs (FA_CNT 0.12% and FA_CNT 0.24%) were selected, since no significant change was observed in samples with low percentages of CNTs.

Initial measurements of the thermal diffusivity values of the un-degassed samples (CNT_FA) and neat asphalt at 40°C showed the presence of CNTs in the asphalt binder decreased its thermal diffusivity, which was against the hypothesis. The 0.24% percentage of CNT-modified foamed asphalt binder showed even lower thermal diffusivity (0.028 mm²/s) than the foamed asphalt (FA). From looking at Figure 17Figure 17 (a), it can be seen that FA has also lower

diffusivity than the neat asphalt (NA). Thus, the authors believe that the presence of the water bubbles inside the asphalt caused a thermal mismatch in the matrix of the asphalt binder, and accordingly, distorted the phonons' free path, which is mainly responsible for the thermal conduction of heat in polymers. In other words, the introduction of an inhomogeneity with lower thermal diffusivity (water bubbles) into the asphalt binder negated the effects of CNTs in the asphalt or even caused a reduction of the final diffusivity values.

To test the above assumption, the foamed samples were degassed in a vacuum oven for 2.5 hours at 135°C to remove all the air bubbles that were trapped inside the binder. The thermal properties of the degassed samples were then tested. The thermal conductivity of the degassed foamed samples and the neat binder at 40°C are shown in Figure 17Figure 17. The thermal conductivity of the CNT modified samples had an increase after degassing, as the conductivity of 0.24% CNT samples is much higher than the foamed (FA) and the neat asphalt (NA). The ratio of the improvement in the values of thermal conductivity in the CNT modified samples compared to the foamed asphalt sample is shown in Figure 17Figure 17 (b).



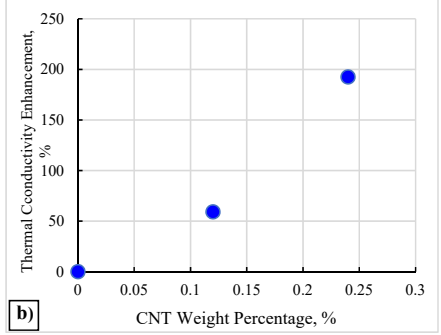


Figure 17 a) Thermal conductivity of the degassed foamed samples and neat binder; b) the relative percentage of enhancement in thermal conductivity.

3.5. Heat capacity and glass transition results from the DSC

Error! Reference source not found. Table 3 shows the heat capacity (C_p) values of the neat binder, the un-degassed and degassed foamed samples. Analysis of the DSC results shows that the degassing process led to a reduction in specific heat capacity C_p values for intermediate and high temperatures for the foamed asphalt (FA), 0.12% CNT FA, and 0.24% CNT FA. For

instance, the degassed foamed binder (FA) had a smaller C_p than the samples without degassing for temperatures above -15°C, and increase in C_p for temperatures below -15°C. This might be because the deionized water has a C_p value of ~3.675 J/g.K, which is more than twice the C_p of the binder at 25°C. The foamed samples likely had water trapped in the sample and the degassing process removed this water content. Therefore, the C_p values of the degassed foamed samples are smaller than those of their un-degassed counterparts. In addition, the C_p values of all the degassed foamed samples are smaller than that of the neat asphalt. The thermal conductivity can be written in terms of $\rho \alpha C_p$ (ρ =density; α =thermal diffusivity). Once the CNT concentration reaches the percolation threshold at ~0.12%, adding more CNTs does not produce consistent enhancement to the effective thermal conductivity.

Table 3 The Specific Heat Capacity and Thermal Diffusivity of All Samples.

Type	Sample	Specific Heat Capacity (J/(g·°C)	Diffusivity (mm ² /s)
	NA	1.541	0.088
	FA	1.470	
Un-degassed	0.12% CNT FA	1.492	
	0.24% CNT FA	1.348	
	FA	1.285	0.173
Degassed	0.12% CNT FA	1.371	0.179
	0.24% CNT FA	1.271	0.227

The glass transition temperature (T_g) of the samples can be assessed from the temperature derivative of the reversing heat capacity curve (i.e., dC_p/dT) as shown in

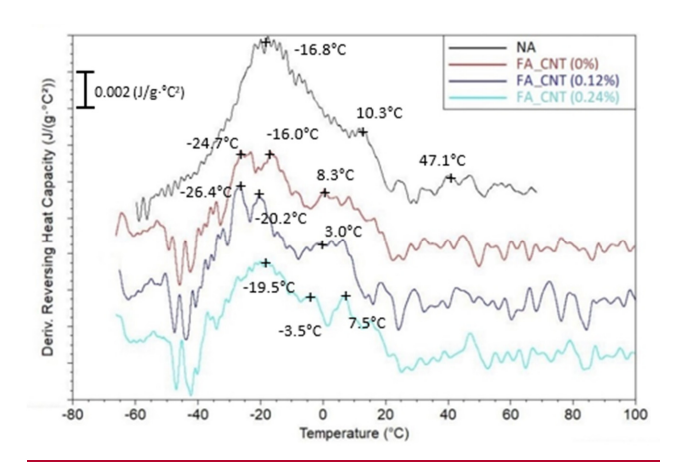


Figure 18 Figure 18. The neat asphalt binder (NA) showed a strong T_g at 16.8° C and two weak T_g s at 10.3° C and 47.1° C, respectively. In contrast, the FA sample had its main T_g split into two Tg's: one at -24.7°C and the other at -16.0°C, followed by a secondary T_g at 8.3° C and other non-obvious glass transitions at a higher temperature. A comparison of the glass transition temperatures suggests that T_g s of the three foamed samples shifted to lower temperatures, which can be caused by the foaming process softening the binder. In addition, samples FA and 0.12% CNT FA had two split T_g s in contrary to the single main T_g in the neat binder. This observation can be related to the addition of the water bubbles into the asphalt binder and changes in the ratio of the chemical composition of the asphalt binder, i.e., saturates, aromatics, resin, and asphaltenes (SARA) fractions, and the corresponding hydrogen to carbon (H/C) ratio, where the bonding at the elemental and molecular level significantly changes.

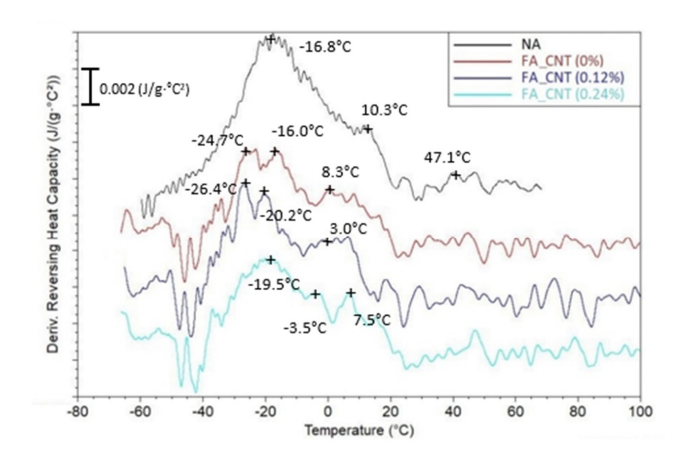


Figure 18 The temperature derivative of the reversing heat capacity (dC_n/dT) for samples.

4. Discussion and Recommendations

The testing results showed that good opportunities exist for incorporating CNTs as a modifier in asphalt binder through the foaming process to improve the foaming performance and binder's thermal properties. The dispersion results of CNTs in ethanol versus in a commercial water-based surfactant revealed that the latter performs better in reducing the agglomerations of CNTs. Moreover, it is safer to use in the mass production of asphalt concrete as ethanol may be flammable and pose fire hazards. Additionally, the CNT modification process can be easily integrated into the existing water-based foaming process. Therefore, the water-based foaming process is recommended for future applications when CNTs need to be incorporated into the asphalt mix.

When using CNTs to modify asphalt binder, it is important to see if CNTs produce any negative impact on the thermomechanical properties or the long-term performance of asphalt concrete. The test results showed that the complex moduli of the asphalt binder did not negatively change after the addition of the CNTs. The specific heat capacity of the foamed samples was smaller than the neat binder; whereas the glass transition temperature of the foamed samples slightly shifted to a lower temperature as compared to that of the neat binder. The thermal conductivity of the 6% CNT sample (0.24% wt. in asphalt) was improved two-fold compared with

the foamed unmodified asphalt. These findings approve the potential of using CNTs in the binder for future applications.

This research shows that the effectiveness of using CNTs in asphalt concrete significantly depends on the uniformity and network formation of CNTs in the asphalt binder. Increasing CNTs in form of agglomeration particles cannot achieve the desirable properties of CNTs in asphalt. To disperse CNTs in water with the surfactant, 6% of CNTs is the maximum content that could be achieved while avoiding agglomeration. When the well-dispersed CNT-water solution is introduced into the foaming process as a foaming agent, overdosing on the foaming agent may cause moisture susceptibility in long-term performance. Typically, 2-3% of water content is recommended [11], which translates to 0.1~0.2% CNTs in the asphalt binder. Considering the percolation threshold of CNT composites is often in a range of 0.05-1% depending on the aspect ratio of CNTs and mixing methods [56-59], it might not be possible to achieve a high enough CNT content to optimize the enhancement of CNTs. In other words, it is not so important to include as much CNTs as possible in the asphalt binder, but rather to consider how well the CNTs are distributed and connected in the network to each other.

5. Conclusions

This paper introduces a new approach to mixing carbon nanotubes (CNTs) through a foaming process to produce high-performance warm mix asphalt (WMA). Specific findings from the morphology, rheology, and thermal parameters of the samples that have been studied are summarized as follows:

- Compared with ethanol, the DI-water surfactant can improve CNT dispersion to obtain a stable CNT-water solution without agglomeration of up to 6% of CNTs.
- The effect of the CNTs on the ER of the foamed asphalt is not significant; nevertheless, the ER slightly decreases as the CNTs proportion increases.
- When 0.1 wt.% of CNTs are added to the foamed asphalt, the HL and FI of the foamed asphalt increase by 45% and 28% respectively compared with the unmodified sample with no CNTs (FA_CNT 0%), which demonstrates that the added CNTs could considerably enhance the overall foaming performance of the foamed asphalt.
- A slight softening effect was observed after the foaming process compared with the neat sample. Once the CNTs were added to the foamed asphalt, their complex modulus gradually increased as the CNTs' proportion increased.

- The failure temperature of the foamed asphalt gradually increases as more CNTs are added
 to the foamed asphalt, indicating that the added CNTs could effectively enhance the
 pavement's resistance to permanent deformation.
- The foaming and the modification with CNT had no negative effect on increasing the stiffness of the neat asphalt binder.
- The specific heat capacity and glass transition temperature of the degassed foamed CNT asphalt binder are reduced in comparison with the neat asphalt binder.
- The thermal conductivity of the CNT_FA (0.24%) sample (6% CNTs in solution) of the
 degassed sample resulted in a two-fold increase in the thermal conductivity compared to
 that of the foamed binder, thus, showing the effectiveness of the carbon nanotubes in
 improving the heat flow transfer in foamed asphalt.

The conclusions made in this paper can be applicable to other asphalt binders. However, it is recommended that more parametric studies be conducted for different asphalt binders to achieve optimal material performance. Future research to develop new surfactants or improve the foaming process may achieve CNT content above the percolation threshold for optimally enhanced performance. Different reinforcements, such as short fibers, can be introduced to asphalt mix production in the same fashion. Moreover, further studies can also be done using other types of binder grading as appropriate for different climates.

6. Acknowledgment

This work is sponsored by the National Science Foundation CMMI 1301160, AF14-AT22, IIP #1738802, IIP # 1941244, and CMMI #1762891, whose support is gratefully acknowledged. The authors would also like to thank the Carleton Laboratory director and staff especially Dr. Liming Li, Mr. Ceaser Jefferson Chabla-Sarmiento, and Mr. Bhumipak Auewarakul for their contributions to the laboratory testing, and Mr. Jeff Xie for his help with manuscript preparation. The contents of this paper reflect the view of the authors, who are responsible for the facts and the accuracy of the data presented. This paper does not constitute a standard, specification, or regulation.

References

- 1. Bower, N., H. Wen, S. Wu, K. Willoughby, J. Weston, and J. DeVol, *Evaluation of the performance of warm mix asphalt in Washington state*. International Journal of Pavement Engineering, 2016. **17**(5): p. 423-434.
- Chowdhury, A. and J.W. Button, A review of warm mix asphalt. Texas Transportation Institute, the Texas A & M University System., 2008.
- 3. Dinis-Almeida, M. and M.L. Afonso, *Warm mix recycled asphalt–a sustainable solution*. Journal of Cleaner Production, 2015. **107**: p. 310-316.
- Ozturk, H.I. and M.E. Kutay, Sensitivity of nozzle-based foamed asphalt binder characteristics to foaming parameters. Transportation Research Record, 2014. 2444(1): p. 120-129.
- 5. Jenkins, K., M. Van de Ven, and J. De Groot. *Characterisation of foamed bitumen*. in 7th Conference on asphalt pavements for Southern Africa. 1999.
- Saleh, M., Characterisation of foam bitumen quality and the mechanical properties of foam stabilised mixes. 2006.
- Arega, Z.A., A. Bhasin, W. Li, D.E. Newcomb, and E. Arambula, *Characteristics of asphalt binders foamed in the laboratory to produce warm mix asphalt.* Journal of Materials in Civil Engineering, 2014. 26(11): p. 04014078.
- 8. Hansen, K.R., A. Copeland, and N.A.P. Association, *Annual asphalt pavement industry survey on recycled materials and warm-mix asphalt usage: 2009-2012.* 2013, National Asphalt Pavement Association.
- 9. Apeagyei, A.K., Evaluating foamed asphalt stability using acoustic emission techniques. Journal of materials in civil engineering, 2013. **25**(9): p. 1291-1298.
- Hailesilassie, B.W., M. Hugener, and M.N. Partl, Influence of foaming water content on foam asphalt mixtures. Construction and Building Materials, 2015. 85: p. 65-77.
- 11. Zhu, S., F. Chen, and H. Yin, Simulation and validation of asphalt foaming process for virtual experiments and optimisation of WMA production. Road Materials and Pavement Design, 2017. 18(sup4): p. 144-164.
- 12. Hasan, M.R.M., Z. You, and X. Yang, *A comprehensive review of theory, development, and implementation of warm mix asphalt using foaming techniques.* Construction and Building Materials, 2017. **152**: p. 115-133.
- 13. Wielinski, J., A. Hand, and D.M. Rausch, *Laboratory and field evaluations of foamed warm-mix asphalt projects*. Transportation Research Record, 2009. **2126**(1): p. 125-131.
- 14. Kuna, K., G. Airey, and N. Thom, *Laboratory mix design procedure for foamed bitumen mixtures*. Transportation Research Record, 2014. **2444**(1): p. 1-10.
- You, Z., J. Mills-Beale, J.M. Foley, S. Roy, G.M. Odegard, Q. Dai, and S.W. Goh, Nanoclay-modified asphalt materials: Preparation and characterization. Construction and Building Materials, 2011. 25(2): p. 1072-1078.
- Abdullah, M.E., K.A. Zamhari, M.R. Hainin, E.A. Oluwasola, N.A. Hassan, and N.I.M. Yusoff, Engineering properties of asphalt binders containing nanoclay and chemical warm-mix asphalt additives. Construction and Building Materials, 2016. 112: p. 232-240.
- Cong, P., P. Xu, and S. Chen, Effects of carbon black on the anti aging, rheological and conductive properties of SBS/asphalt/carbon black composites. Construction and Building Materials, 2014. 52: p. 306-313.

- Tyson, B.M., R.K. Abu Al-Rub, A. Yazdanbakhsh, and Z. Grasley, Carbon nanotubes and carbon nanofibers for enhancing the mechanical properties of nanocomposite cementitious materials. Journal of Materials in Civil Engineering, 2011. 23(7): p. 1028-1035.
- 19. Vo, H.V., D.-W. Park, W.-J. Seo, and B.-S. Yoo, *Evaluation of asphalt mixture modified with graphite and carbon fibers for winter adaptation: Thermal conductivity improvement.* Journal of Materials in Civil Engineering, 2017. **29**(1): p. 04016176.
- Tahami, S.A., A.F. Mirhosseini, S. Dessouky, H. Mork, and A. Kavussi, *The use of high content of fine crumb rubber in asphalt mixes using dry process*. Construction and Building Materials, 2019. 222: p. 643-653.
- Ziari, H. and A. Moniri, Laboratory evaluation of the effect of synthetic Polyolefin-glass fibers on performance properties of hot mix asphalt. Construction and Building Materials, 2019. 213: p. 459-468.
- Zadshir, M., D.J. Oldham, S. Hosseinnezhad, and E.H. Fini, *Investigating bio-rejuvenation mechanisms in asphalt binder via laboratory experiments and molecular dynamics simulation*. Construction and Building Materials, 2018. 190: p. 392-402.
- 23. Li, R., F. Xiao, S. Amirkhanian, Z. You, and J. Huang, *Developments of nano materials and technologies on asphalt materials—A review*. Construction and Building Materials, 2017. **143**: p. 633-648.
- Pan, P., S. Wu, Y. Xiao, P. Wang, and X. Liu, Influence of graphite on the thermal characteristics and anti-ageing properties of asphalt binder. Construction and Building Materials, 2014. 68: p. 220-226.
- He, X., S. Abdelaziz, F. Chen, and H. Yin, Finite element simulation of self-heated pavement under different mechanical and thermal loading conditions. Road Materials and Pavement Design, 2019. 20(8): p. 1807-1826.
- 26. Yu, X., M. Zadshir, J.R. Yan, and H. Yin, *Morphological, thermal, and mechanical properties of asphalt binders modified by graphene and carbon nanotubes*. ASCE Journal of Materials in Civil Engineering (In publication).
- 27. Treacy, M.J., T.W. Ebbesen, and J.M. Gibson, *Exceptionally high Young's modulus observed for individual carbon nanotubes*. nature, 1996. **381**(6584): p. 678-680.
- 28. De Heer, W.A., *Nanotubes and the pursuit of applications*. MRS bulletin, 2004. **29**(4): p.
- 29. Baughman, R.H., A.A. Zakhidov, and W.A. De Heer, *Carbon nanotubes--the route toward applications*. science, 2002. **297**(5582): p. 787-792.
- Xiao, F., A.N. Amirkhanian, and S.N. Amirkhanian, Influence of carbon nanoparticles on the rheological characteristics of short-term aged asphalt binders. Journal of Materials in Civil Engineering, 2011. 23(4): p. 423-431.
- Khattak, M.J., A. Khattab, H.R. Rizvi, and P. Zhang, The impact of carbon nano-fiber modification on asphalt binder rheology. Construction and Building Materials, 2012. 30: p. 257-264.
- Santagata, E., O. Baglieri, L. Tsantilis, and D. Dalmazzo, Rheological characterization of bituminous binders modified with carbon nanotubes. Procedia-Social and Behavioral Sciences, 2012. 53: p. 546-555.
- 33. Motlagh, A.A., A. Kiasat, E. Mirzaei, and F.O. Birgani, *Bitumen modification using carbon nanotubes*. World Applied Sciences Journal, 2012. **18**(4): p. 594-599.

- 34. Amin, I., S.M. El-Badawy, T. Breakah, and M.H. Ibrahim, *Laboratory evaluation of asphalt binder modified with carbon nanotubes for Egyptian climate*. Construction and Building Materials, 2016. **121**: p. 361-372.
- 35. Amirkhanian, A.N., F. Xiao, and S.N. Amirkhanian, *Characterization of unaged asphalt binder modified with carbon nano particles*. International Journal of Pavement Research and Technology, 2011. **4**(5): p. 281.
- Amirkhanian, A.N., F. Xiao, and S.N. Amirkhanian, Evaluation of high temperature rheological characteristics of asphalt binder with carbon nano particles. Journal of Testing and Evaluation, 2011. 39(4): p. 1.
- 37. Santagata, E., O. Baglieri, L. Tsantilis, and G. Chiappinelli, *Fatigue properties of bituminous binders reinforced with carbon nanotubes*. International Journal of Pavement Engineering, 2015. **16**(1): p. 80-90.
- Ziari, H., A. Amini, A. Goli, and D. Mirzaiyan, Predicting rutting performance of carbon nano tube (CNT) asphalt binders using regression models and neural networks.
 Construction and Building Materials, 2018. 160: p. 415-426.
- 39. Ameri, M., S. Nowbakht, M. Molayem, and M. Aliha, *Investigation of fatigue and fracture properties of asphalt mixtures modified with carbon nanotubes.* Fatigue & fracture of engineering materials & structures, 2016. **39**(7): p. 896-906.
- 40. Wang, P., Z.-j. Dong, Y.-q. Tan, and Z.-y. Liu, Effect of multi-walled carbon nanotubes on the performance of styrene-butadiene-styrene copolymer modified asphalt. Materials and Structures, 2017. **50**(1): p. 1-11.
- 41. Mamun, A., M. Arifuzzaman, and R. Taha, *Nano scale aging characterization of carbon nanotube modified asphalt binders*. Proceedings of the Advances in Materials and Pavement Performance Prediction, 2018: p. 403-406.
- 42. Xie, X.-L., Y.-W. Mai, and X.-P. Zhou, *Dispersion and alignment of carbon nanotubes in polymer matrix: a review.* Materials science and engineering: R: Reports, 2005. **49**(4): p. 89-112.
- 43. Hasan, Z., R.-o. Kamran, F. Mohammad, G. Ahmad, and F. Hosein, *Evaluation of different conditions on the mixing bitumen and carbon nano-tubes*. International Journal of Civil & Environmental Engineering IJCEE-IJENS, 2012. **12**(06): p. 53-59.
- 44. Faramarzi, M., M. Arabani, A. Haghi, and V. Mottaghitalab, *Carbon Nanotubes-modified Asphalt Binder: Preparation and Characterization*. International Journal of Pavement Research & Technology, 2015. **8**(1).
- 45. Latifi, H. and P. Hayati, Evaluating the effects of the wet and simple processes for including carbon Nanotube modifier in hot mix asphalt. Construction and Building Materials, 2018. **164**: p. 326-336.
- 46. Bai, J. and A. Allaoui, Effect of the length and the aggregate size of MWNTs on the improvement efficiency of the mechanical and electrical properties of nanocomposites—experimental investigation. Composites Part A: applied science and manufacturing, 2003. 34(8): p. 689-694.
- 47. Yu, A., M.E. Itkis, E. Bekyarova, and R.C. Haddon, *Effect of single-walled carbon nanotube purity on the thermal conductivity of carbon nanotube-based composites*. Applied Physics Letters, 2006. **89**(13): p. 133102.
- Brennen, M., M. Tia, A. Altschaeffl, and L. Wood, Laboratory investigation of the use of foamed asphalt for recycled bituminous pavements. Transportation Research Record, 1983(911).

- 49. Schwartz, C.W. and S. Khosravifar, *Design and evaluation of foamed asphalt base materials*. 2013, Maryland. State Highway Administration. Office of Policy & Research.
- 50. Namutebi, M., *Some aspects of foamed bitumen technology*. 2011, KTH Royal Institute of Technology.
- 51. Ozturk, H.I., Quantification of quality of foamed warm mix asphalt binders and mixtures. 2013: Michigan State University.
- 52. Jenkins, K.J., Mix design considerations for cold and half-warm bituminous mixes with emphasis of foamed bitumen. 2000, Stellenbosch: Stellenbosch University.
- Masson, J., G. Polomark, and P. Collins, Time-dependent microstructure of bitumen and its fractions by modulated differential scanning calorimetry. Energy & Fuels, 2002. 16(2): p. 470-476.
- Martinez-Arguelles, G., F. Giustozzi, M. Crispino, and G.W. Flintsch, *Investigating physical and rheological properties of foamed bitumen*. Construction and Building Materials, 2014. 72: p. 423-433.
- 55. Yu, X., S. Liu, and F. Dong, Comparative assessment of rheological property characteristics for unfoamed and foamed asphalt binder. Construction and Building Materials, 2016. **122**: p. 354-361.
- Jang, S.H. and H.M. Yin, Effective electrical conductivity of carbon nanotube-polymer composites: a simplified model and its validation. Materials Research Express, 2015. 2(4).
- 57. Jang, S.H., D.P. Hochstein, S. Kawashima, and H.M. Yin, *Experiments and micromechanical modeling of electrical conductivity of carbon nanotube/cement composites with moisture*. Cement & Concrete Composites, 2017. 77: p. 49-59.
- 58. Yum, S.G., H. Yin, and S.H. Jang, *Toward Multi-Functional Road Surface Design with the Nanocomposite Coating of Carbon Nanotube Modified Polyurethane: Lab-Scale Experiments.* Nanomaterials, 2020. **10**(10).
- Li, J., P.C. Ma, W.S. Chow, C.K. To, B.Z. Tang, and J.K. Kim, Correlations between percolation threshold, dispersion state, and aspect ratio of carbon nanotubes. Advanced Functional Materials, 2007. 17(16): p. 3207-3215.